CHAPTER 12

FUNDAMENTAL CONCEPTS REGARDING DEEP FOUNDATIONS UNDER LATERAL LOADING

12.1 INTRODUCTION

12.1.1 Description of the Problem

A pile subjected to lateral loading is one of a class of problems that involve the interaction of soils and structures. Soil–structure interaction is encountered in every problem in foundation engineering, but in some cases the structure is so stiff that a solution can be developed assuming nonlinear behavior for the soil and no change in shape for the structural unit. But for a pile under lateral loading, a solution cannot be obtained without accounting for the deformation of both the pile and the soil. The deflection of the pile and the lateral resistance of the soil are interdependent; therefore, because of the nonlinearity of the soil, and sometimes of the pile, iterative techniques are almost always necessary to achieve a solution for a particular case of loading on the pile.

This chapter is aimed at developing an understanding of soil–structure interaction as related to the single pile. Many structures are supported by groups of piles, and methods of analyzing such groups will be presented in Chapter 15. However, the methods of analysis of pile groups under lateral loading begin with the analysis of single piles; soil response are then modified according to pile spacing. While this chapter describes the nature of the problem of the laterally loaded pile and presents a useful method of analysis, Chapter 15 presents comprehensive methods of analysis of single piles and utilizes them in the analysis of groups.

12.1.2 Occurrence of Piles Under Lateral Loading

As noted below, a principal use of piles is to support offshore platforms. A system of design and construction is employed to minimize the length of time

that an expensive derrick barge with special equipment and personnel is needed at the site. A jacket or template is constructed onshore, floated to the site or transported on a barge, and placed on the ocean floor by the derrick barge. One or more soil borings are made from a special rig prior to construction. Prefabricated piles of open-ended steel pipe are stabbed into slots in the template and driven into position with an impact hammer. The piles are designed to achieve the desired axial load with the largest wall thickness in the area of computed maximum moment, usually near the mudline, and problems arise if the piles cannot be driven to the required depth. Sometimes a smaller-diameter pile is placed to the needed penetration by drilling and grouting, with a sizable increase in cost. Other problems arise if a pile is damaged during the stabbing operation and cannot be driven to the necessary depth. The system, however, has been used successfully at hundreds of offshore locations around the world.

A view of an offshore drilling platform in the Gulf of Mexico from a helicopter is presented in Figure 12.1. The helipad is shown. Helicopters are used for much of the transport of personnel at the offshore location. An interesting feature in the design of fixed offshore platforms is the distance the deck is raised above the water surface. A distance designed to be above the crest of the largest wave is expected. The projected area of the members below the deck is relatively austere, with the purpose of minimizing the forces generated by waves during a hurricane.

Another important use of piles under lateral loading is to support overhead structures sustaining a variety of facilities. Examples are wind farms, trans-

Figure 12.1 Helicopter view of an offshore drilling platform in the Gulf of Mexico.

mission lines, microwave towers, highways, signs, and a variety of units in industrial plants. A view of wind turbines that form a wind farm is presented in Figure 12.2. The height of the tower can range from 22 to 80 m, with a rotor diameter of up to 76 m. The largest turbine can generate power of up to 2000 kW (DNV/Risø, 2001). The environmental characteristics of a wind farm may be understood by viewing the grazing cow in the right foreground of the photograph.

Many pile-supported bridges are subjected to wind and forces from storm water. A special problem is impact from floating vessels. Some high-rise buildings are subjected to large lateral forces from wind, earthquakes, and sometimes from earth pressure.

12.1.3 Historical Comment

Pile-supported structures in the past were frequently subjected to lateral loading, but the piles were designed by using judgment or by referring to building codes, which usually allowed a modest load on each pile if the soil met certain conditions. Designs became more critical when platforms were built offshore in the Gulf of Mexico by the oil industry or off the East Coast of the United States by the Federal government to support early-warning radar equipment.

Engineers understood early that a pile under lateral load would act as a beam. Hetenyi (1946) wrote a book giving the solution of the differential equation for a beam on a foundation, with a linear relationship between pile deflection and soil response. In the early 1950s, Shell Oil Company was planning to install an offshore platform at Block 42 in 25 m (82 ft) of water near the Louisiana coast, where the soil was predominantly soft clay. A pro-

Figure 12.2 View of a wind farm at an onshore location.

cedure was available for computing lateral forces on the platform during a hurricane. Two groups of engineers were asked to work independently and compute the deflection and bending stresses for the pipe piles supporting the platform. One team used the work of Hetenyi, and the other team used limit analysis to obtain the reaction from the soft clay at the site and estimated the pile response. The answers varied widely, and a joint meeting revealed that research was needed on predicting *p-y* curves.

A comprehensive research program was initiated by Shell, and joined later by other companies, for two parallel developments: (1) methods for predicting *p-y* curves and (2) techniques for solving the relevant differential equation. Much of the Shell research was released in time and has been followed by contributions from many investigators. Research is continuing, but given here is practical information for understanding the nature of the problem and for obtaining solutions for some particular cases.

12.2 DERIVATION OF THE DIFFERENTIAL EQUATION

In most instances, the axial load on a laterally loaded pile has relatively little influence on bending moment. However, there are occasions when it is desirable to find the buckling load for a pile; thus, the axial load is needed in the derivation. The derivation for the differential equation for the beam column on a foundation was given by Hetenyi (1946).

The assumption is made that a bar on an elastic foundation is subjected to horizontal loading and to a pair of compressive forces P_x acting in the center of gravity of the end cross sections of the bar. If an infinitely small unloaded element, bounded by two horizontals a distance dx apart, is cut out of this bar (see Figure 2.1), the equilibrium of moments (ignoring second-order terms) leads to the equation

$$(M + dM) - M + P_x dy - V_v dx = 0 \tag{12.1}$$

or

$$\frac{dM}{dx} + P_x \frac{dy}{dx} - V_v = 0 \tag{12.2}$$

Differentiating Eq. 12.2 with respect to x, the following equation is obtained:

$$\frac{d^2M}{dx^2} + P_x \frac{d^2y}{dx^2} - \frac{dV_v}{dx} = 0. \tag{12.3}$$

The following identities are noted:

$$\frac{d^2M}{dx^2} = E_p I_p \frac{d^4y}{dx^4}$$

$$\frac{dV_v}{dx} = p$$

and

$$p = E_{py} y$$

And making the indicated substitutions, Eq. 12.3 becomes

$$E_p I_p \frac{d^4y}{dx^4} + P_x \frac{d^2y}{dx^2} + E_{py} y = 0 \tag{12.4}$$

The direction of the shearing force V_v is shown in Figure 12.3. The shearing force in the plane normal to the deflection line can be obtained as follows:

$$V_n = V_v \cos S - P_x \sin S \tag{12.5}$$

Because S is usually small, cos S = 1 and sin S = tan S = dy/dx. Thus, Eq. 12.6 is obtained:

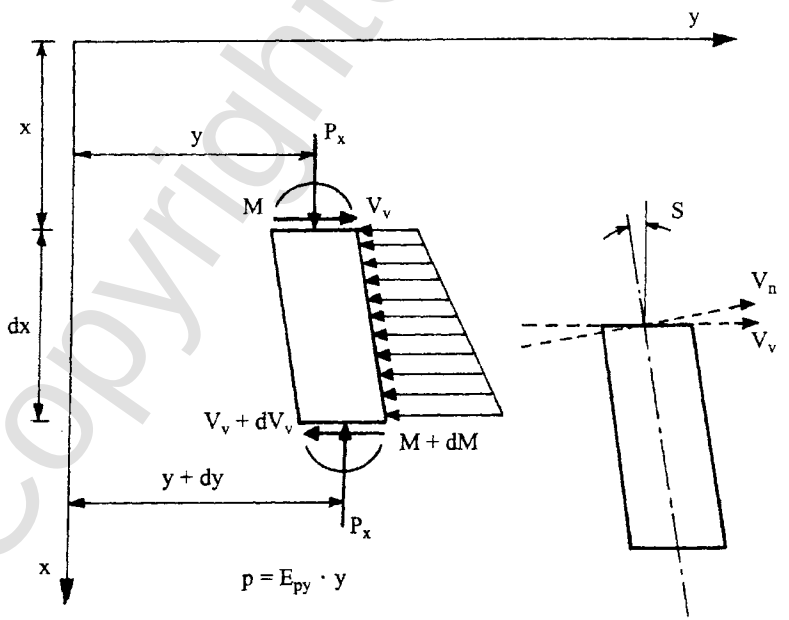

Figure 12.3 Element from a beam column (after Hetenyi, 1946).

$$V_n = V_v - P_x \frac{dy}{dx} \tag{12.6}$$

V_n will be used mostly in computations, but V_v can be computed from Eq. 12.6, where dy/dx is equal to the rotation S.

The ability to allow a distributed force W per unit of length along the upper portion of a pile is convenient in solving a number of practical problems. The differential equation is then given by Eq. 12.7:

$$E_p I_p \frac{d^4}{dx^4} + P_x \frac{d^2y}{dx^2} - p + W = 0 \tag{12.7}$$

where

P_x = axial load on the pile,
y = lateral deflection of the pile at a point x along the length of the pile,
p = soil reaction per unit length,
$E_p I_p$ = bending stiffness, and
W = distributed load along the length of the pile.

Other beam formulas that are needed in analyzing piles under lateral loads are:

$$E_p I_p \frac{d^3y}{dx^3} + P_x \frac{dy}{dx} = V \tag{12.8}$$

$$E_p I_p \frac{d^2y}{dx^2} = M \tag{12.9}$$

$$\frac{dy}{dx} = S \tag{12.10}$$

where

V = shear in the pile,
M = bending moment of the pile, and
S = slope of the elastic curve defined by the axis of the pile.

Except for the axial load P_x, the sign conventions are the same as those usually employed in the mechanics for beams, with the axis for the pile rotated 90° clockwise from the axis for the beam. The axial load P_x does not normally appear in the equations for beams. The sign conventions are pre-

sented graphically in Figure 12.4. A solution of the differential equation yields a set of curves such as those shown in Figure 12.5. The mathematical relationships for the various curves that give the response of the pile are shown in the figure for the case where no axial load is applied.

The assumptions that are made in deriving the differential equation are as follows:

1. The pile is straight and has a uniform cross section.
2. The pile has a longitudinal plane of symmetry; loads and reactions lie in that plane.

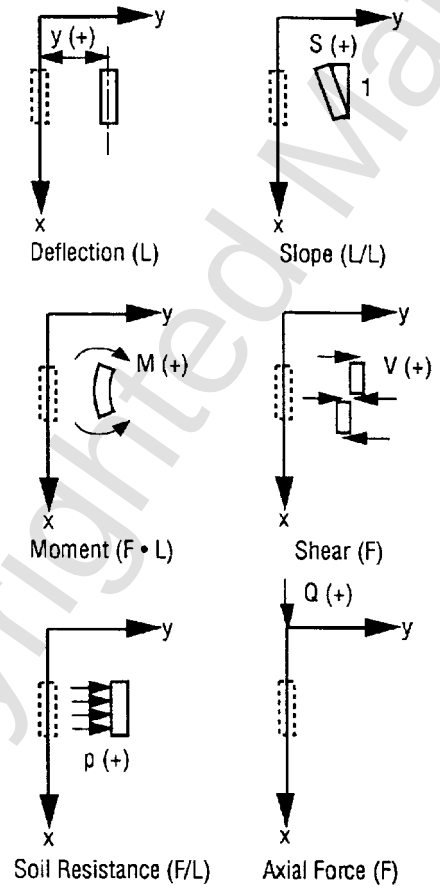

Note: All of the responses of the pile and soil are shown in the positive sense; F = Force; L = Length.

Figure 12.4 Sign conventions for a pile under lateral loading.

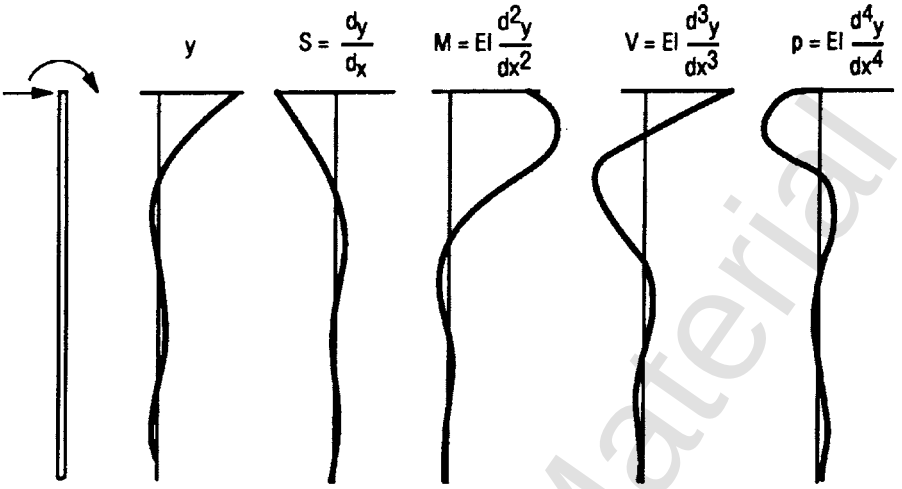

Figure 12.5 Form of the results obtained from a complete solution.

3. The pile material is homogeneous and isotropic.
4. The proportional limit of the pile material is not exceeded.
5. The modulus of elasticity of the pile material is the same in tension and compression.
6. Transverse deflections of the pile are small.
7. The pile is not subjected to dynamic loading.
8. Deflections due to shearing stresses are small.

Assumption 8 can be addressed by including more terms in the differential equation, but errors associated with omission of these terms are usually small. The numerical method presented later can deal with the behavior of a pile made of materials with nonlinear stress-strain properties.

12.2.1 Solution of the Reduced Form of the Differential Equation

A simpler form of the differential equation results from Eq. 12.4 if the assumptions are made that no axial load is applied, that the bending stiffness $E_p I_p$ is constant with depth, and that the soil reaction E_{py} is a constant and equal to α. The first two assumptions can be satisfied in many practical cases; however, the third assumption is seldom satisfied in practice.

The solution shown in this section is presented for two important reasons: (1) the resulting equations demonstrate several factors that are common to any solution; thus, the nature of the problem is revealed; and (2) the closed-form solution allows for a check of the accuracy of the numerical solutions given later in this chapter.

If the assumptions shown above and the identity shown in Eq. 12.11 are employed, a reduced form of the differential equation is shown in Eq. 12.12:

$$\beta^4 = \frac{\alpha}{4E_pI_p} \tag{12.11}$$

$$\frac{d^4y}{dx^4} + 4\beta^4 y = 0 \tag{12.12}$$

The solution to Eq. 12.12 may be directly written as

$$y = e^{\beta x}(\chi_1 \cos \beta x + \chi_2 \sin \beta x) + e^{-\beta x}(\chi_3 \cos \beta x - \chi_4 \sin \beta x) \tag{12.13}$$

The coefficients χ_1, χ_2, χ_3, and χ_4 must be evaluated for the various boundary conditions that are desired. If one considers a long pile, a simple set of equations can be derived. An examination of Eq. 12.13 shows that χ_1 and χ_2 must approach zero for a long pile because the term $e^{\beta x}$ will be large with large values of x.

The sketches in Figure 12.6 show the boundary conditions for the top of the pile employed in the reduced form of the differential equations. A more complete discussion of boundary conditions is presented in the next section. The boundary conditions at the top of the long pile that are selected for the first case are illustrated in Figure 12.6a and in equation form are

$$\text{At } x = 0: \quad \frac{d^2y}{dx^2} = \frac{M_t}{E_pI_p} \tag{12.14}$$

$$\frac{d^3y}{dx^3} = \frac{P_t}{E_pI_p} \tag{12.15}$$

From Eq. 12.13 and substitution of Eq. 12.14, one obtains for a long pile

$$\chi_4 = \frac{-M_t}{2E_pI_p\beta^2} \tag{12.16}$$

The substitutions indicated by Eq. 12.15 yield the following:

$$\chi_3 + \chi_4 = \frac{P_t}{2E_pI_p\beta^3} \tag{12.17}$$

Equations 12.16 and 12.17 are used, and expressions for deflection y, slope S, bending moment M, shear V, and soil resistance p for the long pile can be written in Eqs. 12.18 through 12.22:

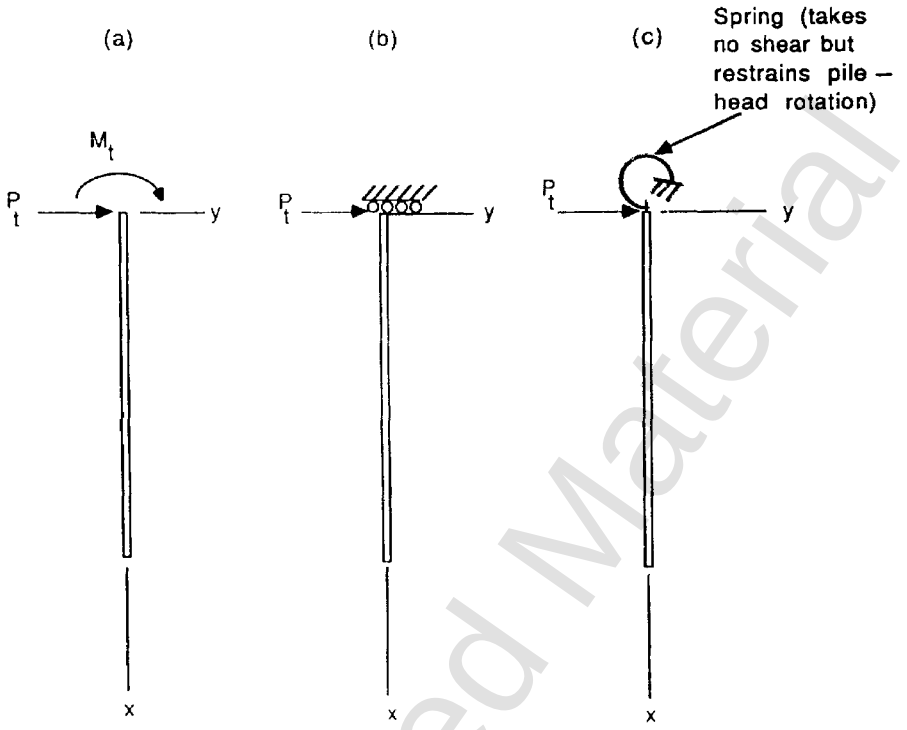

Figure 12.6 Boundary conditions at the top of a pile: (a) free-head. (b) fixed-head. (c) partially restrained.

$$y = \frac{2\beta^2 e^{-\beta x}}{\alpha}\left[\frac{P_t}{\beta}\cos\beta x + M_t(\cos\beta x - \sin\beta x)\right] \tag{12.18}$$

$$S = e^{-\beta x}\left[\frac{2P_t\beta^2}{\alpha}(\sin\beta x + \cos\beta x) + \frac{M_t}{E_pI_p\beta}\cos\beta x\right] \tag{12.19}$$

$$M = e^{-\beta x}\left[\frac{P_t}{\beta}\sin\beta x + M_t(\sin\beta x + \cos\beta x)\right] \tag{12.20}$$

$$V = e^{-\beta x}[P_t(\cos\beta x - \sin\beta x) - 2M_t\beta\sin\beta x] \tag{12.21}$$

$$p = -\beta^2 e^{-\beta x}\left[\frac{P_t}{\beta}\cos\beta x + M_t(\cos\beta x - \sin\beta x)\right] \tag{12.22}$$

It is convenient to define some functions for simplifying the written form of the above equations:

$$A_1 = e^{-\beta x}(\cos \beta x + \sin \beta x) \tag{12.23}$$

$$B_1 = e^{-\beta x}(\cos \beta x - \sin \beta x) \tag{12.24}$$

$$C_1 = e^{-\beta x} \cos \beta x \tag{12.25}$$

$$D_1 = e^{-\beta x} \sin \beta x \tag{12.26}$$

Using these functions, Eqs. 12.18 through 12.22 become

$$y = \frac{2P_t\beta}{\alpha} C_1 + \frac{M_t}{2E_pI_p\beta^2} B_1 \tag{12.27}$$

$$S = \frac{2P_t\beta^2}{\alpha} A_1 - \frac{M_t}{E_pI_p\beta} C_1 \tag{12.28}$$

$$M = \frac{P_t}{\beta} D_1 + M_t A_1, \tag{12.29}$$

$$V = P_t B_1 - 2M_t\beta D_1, \text{ and} \tag{12.30}$$

$$p = -2P_t\beta C_1 - 2M_t\beta^2 B_1. \tag{12.31}$$

Values for A_1, B_1, C_1, and D_1, are shown in Table 12.1 as a function of the nondimensional distance βx along the long pile.

For a long pile whose head is fixed against rotation, as shown in Figure 12.6b, the solution may be obtained by employing the boundary conditions given in Eqs. 12.32 and 12.33:

$$\text{At } x = 0: \quad \frac{dy}{dx} = 0 \tag{12.32}$$

$$\frac{d^3y}{dx^3} = \frac{P_t}{E_pI_p} \tag{12.33}$$

Using the same procedures as for the first set of boundary conditions, the results are as follows:

$$\chi_3 = \chi_4 = \frac{P_t}{4E_pI_p\beta^3} \tag{12.34}$$

The solution for long piles, finally, is given in Eqs. 12.35 through 12.39:

TABLE 12.1 Table of Functions for a Pile of Infinite Length

βx	A_1	B_1	C_1	D_1
0	1.0000	1.0000	1.0000	0.0000
0.1	0.9907	0.8100	0.9003	0.0903
0.2	0.9651	0.6398	0.8024	0.1627
0.3	0.9267	0.4888	0.7077	0.2189
0.4	0.8784	0.3564	0.6174	0.2610
0.5	0.8231	0.2415	0.5323	0.2908
0.6	0.7628	0.1431	0.4530	0.3099
0.7	0.6997	0.599	0.3798	0.3199
0.8	0.6354	−0.0093	0.3131	0.3223
0.9	0.5712	−0.0657	0.2527	0.3185
1.0	0.5083	−0.1108	0.1988	0.3096
1.1	0.4476	−0.1457	0.1510	0.2967
1.2	0.3899	−0.1716	0.1091	0.2807
1.3	0.3355	−0.1897	0.0729	0.2626
1.4	0.2849	−0.2011	0.0419	0.2430
1.5	0.2384	−0.2068	0.0158	0.2226
1.6	0.1959	−0.2077	−0.0059	0.2018
1.7	0.1576	−0.2047	−0.0235	0.1812
1.8	0.1234	−0.1985	−0.0376	0.1610
1.9	0.0932	−0.1899	−0.0484	0.1415
2.0	0.0667	−0.1794	−0.0563	0.1230
2.2	0.0244	−0.1548	−0.0652	0.0895
2.4	−0.0056	−0.1282	−0.0669	0.0613
2.6	−0.0254	−0.1019	−0.0636	0.0383
2.8	−0.0369	−0.0777	−0.0573	0.0204
3.2	−0.0431	−0.0383	−0.0407	−0.0024
3.6	−0.0366	−0.0124	−0.0245	−0.0121
4.0	−0.0258	0.0019	−0.0120	−0.0139
4.4	−0.0155	0.0079	−0.0038	−0.0117
4.8	−0.0075	0.0089	0.0007	−0.0082
5.2	−0.0023	0.0075	0.0026	−0.0049
5.6	0.0005	0.0052	0.0029	−0.0023
6.0	0.0017	0.0031	0.0024	−0.0007
6.4	0.0018	0.0015	0.0017	0.0003
6.8	0.0015	0.0004	0.0010	0.0006
7.2	0.0011	−0.00014	0.00045	0.00060
7.6	0.00061	−0.00036	0.00012	0.00049
8.0	0.00028	−0.00038	−0.0005	0.00033
8.4	0.00007	−0.00031	−0.00012	0.00019
8.8	−0.00003	−0.00021	−0.00012	0.00009
9.2	−0.00008	−0.00012	−0.00010	0.00002
9.6	−0.00008	−0.00005	−0.00007	−0.00001
10.0	−0.00006	−0.00001	−0.00004	−0.00002

$$y = \frac{P_t \beta}{\alpha} A_1 \tag{12.35}$$

$$S = \frac{P_t}{2E_p I_p \beta^2} D_1 \tag{12.36}$$

$$M = -\frac{P_t}{2\beta} B_1 \tag{12.37}$$

$$V = P_t C_1 \tag{12.38}$$

$$p = -P_t \beta A_1 \tag{12.39}$$

It is sometimes convenient to have a solution for a third set of boundary conditions, as shown in Figure 12.6c. These boundary conditions are given in Eqs. 12.40 and 12.41:

$$\text{At } x = 0: \quad \frac{E_p I_p \dfrac{d^2y}{dx^2}}{\dfrac{dy}{dx}} = \frac{M_t}{S_t} \tag{12.40}$$

$$\frac{d^3y}{dx^3} = \frac{P_t}{E_p I_p} \tag{12.41}$$

Employing these boundary conditions, for the long pile the coefficients χ_3 and χ_4 were evaluated and the results are shown in Eqs. 12.42 and 12.43. For convenience in writing, the rotational restraint M_t/S_t is given the symbol k_θ.

$$\chi_3 = \frac{P_t(2E_p I_p + k_\theta)}{E_p I_p(\alpha + 4\beta^3 k_\theta)} \tag{12.42}$$

$$\chi_4 = \frac{k_\theta P_t}{E_p I_p(\alpha + 4\beta^3 k_\theta)} \tag{12.43}$$

These expressions can be substituted into Eq. 12.13 and differentiation performed as appropriate. Substitution of Eqs. 12.23 through 12.26 will yield a set of expressions for the long pile similar to those in Eqs. 12.27 through 12.31 and 12.35 through 12.39.

Timoshenko (1941) stated that the solution for the long pile is satisfactory where $\beta L \geq 4$; however, there are occasions when the solution of the reduced differential equation is desired for piles that have a nondimensional length less than 4. The solution at any pile length L can be obtained by using the following boundary conditions at the tip of the pile:

$$\text{At } x = L: \quad \frac{d^2y}{dx^2} = 0 \quad (M \text{ is zero at pile tip}) \tag{12.44}$$

$$\text{At } x = L: \quad \frac{d^3y}{dx^3} = 0 \quad (V \text{ is zero at pile tip}) \tag{12.45}$$

When the above boundary conditions are fulfilled, along with a set for the top of the pile, the four coefficients χ_1, χ_2, χ_3, and χ_4 can be evaluated.

The influence of the length of a pile on the groundline deflection is illustrated in Figure 12.7. A pile with loads applied is shown in Figure 12.7a; an axial load is shown, but the assumption is made that this load is small, so the lateral load P_t and the moment M_t will control the length of the pile. Computations are made with constant loading, constant pile cross section, and an initial length in the long-pile range. The computations proceed with the length being reduced in increments; the groundline deflection is plotted as a function of the selected length, as shown in Figure 12.7b. The figure shows that the groundline deflection is unaffected until the critical length is approached. At

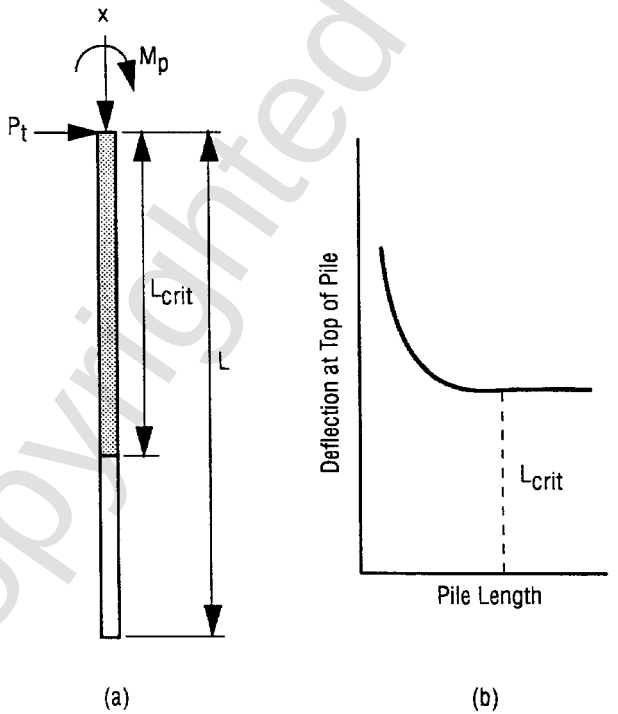

Figure 12.7 Critical length of a pile under lateral loads: (a) pile geometry and loads. (b) pile-head deflection vs. pile length.

this length, only one point of zero deflection will occur in the computations. There will be a significant increase in the groundline deflection as the length in the solution is made less than critical. The engineer can select a length that will give an appropriate factor of safety against excessive groundline deflection. The accuracy of the solution will depend, of course, on how well the soil-response curves reflect the actual situation in the field.

The reduced form of the differential equation will not normally be used for the solution of problems encountered in design. However, the influence of pile length, pile stiffness, and other parameters is illustrated with clarity.

12.3 RESPONSE OF SOIL TO LATERAL LOADING

The above discussion suggests that the key to determining the behavior of a pile under lateral loading is the ability to develop a family of curves (*p-y* curves) that give soil reaction as a function of the lateral deflection of a pile. The nature of *p-y* curves may be understood by referring to Figure 12.8, where a slice of soil is examined (Reese, 1983). Figure 12.6b shows a uniform distribution of unit stresses with units of F/L^2 around a cylindrical pile at some depth z_1 below the ground surface, assuming that the pile was installed without bending. If the pile is assumed to be moved laterally through a distance y_1 (exaggerated in the figure for ease of presentation), the distribution of stresses after the deflection is symmetrical but no longer uniform (Figure 12.8c). The stresses on the side in the direction of movement (front side) have increased, and those on the back side have decreased. Integration of the unit stresses in Figure 12.8c yields the value of p_1 that acts in a direction opposite the deflection y and is called the *soil resistance* or *soil reaction,* with units for force per unit of pile length (F/L). The soil resistance p is similar in concept to the distributed loading encountered in designing a beam supporting a floor slab. Reflection shows that, for the particular value of z below the ground surface, the value of p will vary with the deflection y of the pile and with the kind of soil into which the pile is installed, p_{ult}.

A pile subjected to an axial load, a lateral load, and a moment is shown in Figure 12.9a. A possible shape of the deflected pile is shown in Figure 12.9b, along with a set of nonlinear mechanisms that serve to resist the deflection. A set of *p-y* curves is shown in Figure 12.9c, representing the response of the soil as simulated by the mechanisms. Procedures for predicting *p-y* curves in a variety of soils and rocks are given in Chapter 14; however, the information here demonstrates the method and leads to practical solutions for a class of problems.

The shape of a *p-y* curve conceptually is shown in Figure 12.10. An initial straight-line portion and a final straight-line portion, p_{ult}, define the curve. The two lines are connected by a curve. By referring to Figure 12.8, one can reason that at small deflections, the initial slope of the *p-y* curve should be

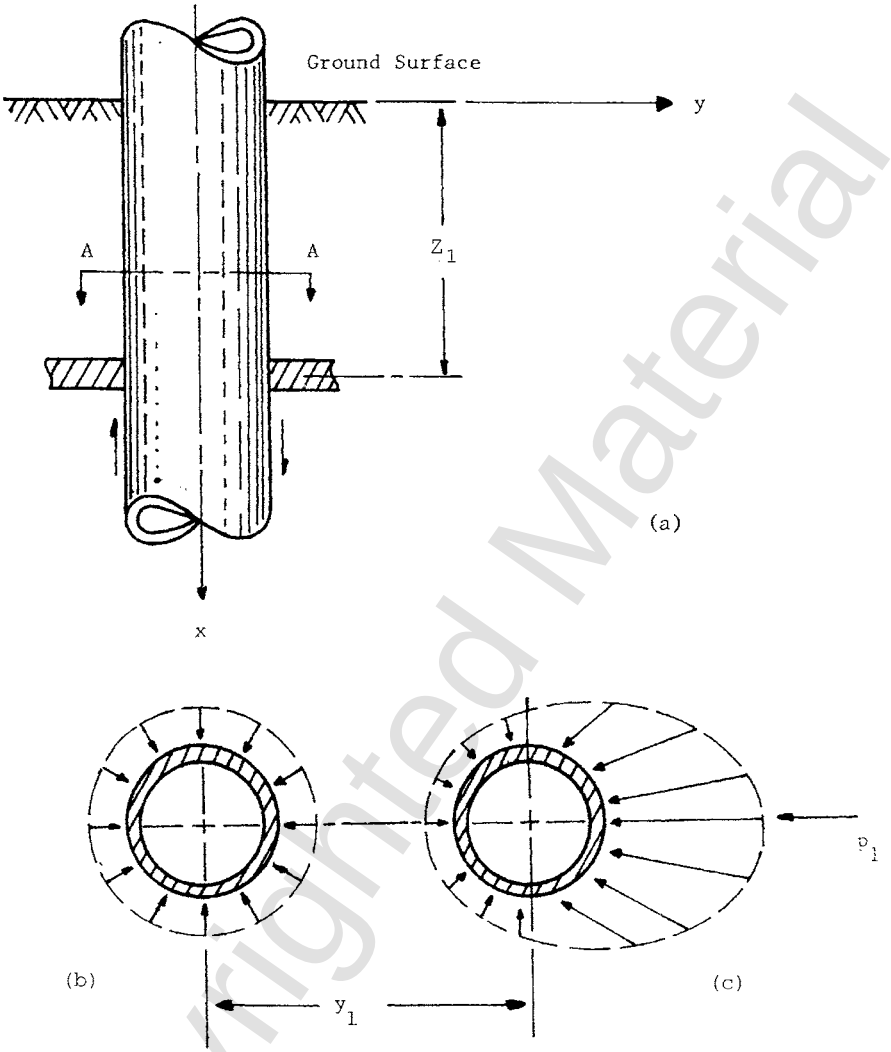

Figure 12.8 Distribution of unit stresses against a pile before and after lateral deflection: (a) elevation view of section of pile. (b) earth pressure prior to lateral loading. (c) earth pressure after lateral loading.

related in some direct way to the initial modulus of the stress-strain curve for the soil. Further, the value of p_{ult} should be related in some direct way to the failure of the soil in bearing capacity.

Figure 12.10 shows a dashed line labeled E_{py}, a secant to the *p*-*y* curve that will be implemented in the analyses that follow. As shown in the figure, E_{py} will have the greatest value with small values of *y* and will decrease with

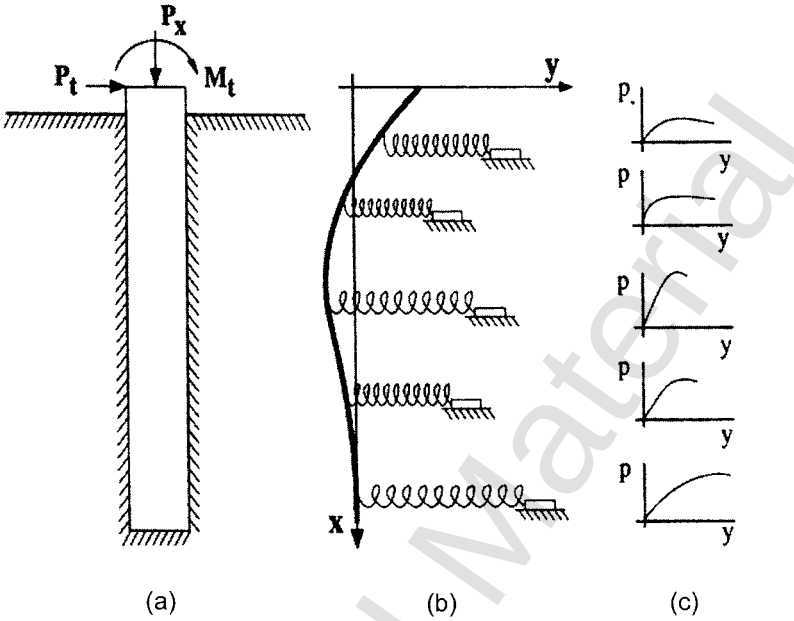

Figure 12.9 Model of a pile subjected to lateral loading with a set of *p-y* curves: (a) pile under lateral loading. (b) soil spring model. (c) *p-y* curves.

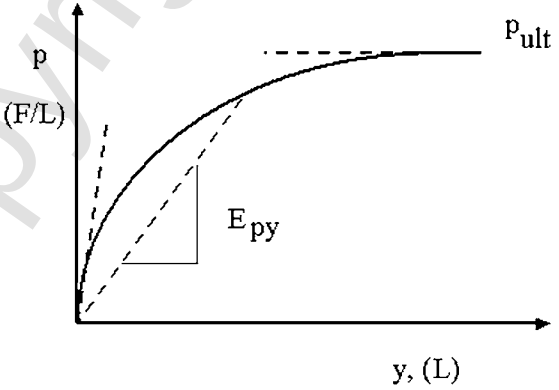

Figure 12.10 Conceptual shape of a *p-y* curve.

increasing pile deflection. Because of the nonlinearity of the response of the soil to deflection, a solution must proceed for a given pile and a given set of loadings by selecting trial values of E_{py}, solving a set of equations for deflection of the pile, obtaining improved values of E_{py}, and continuing until convergence is achieved. The computer solves such a problem with ease, but hand solutions are also available, as shown later in this chapter.

12.4 EFFECT OF THE NATURE OF LOADING ON THE RESPONSE OF SOIL

Four types of loading can be defined as affecting the response of soil around a pile when loaded laterally: short-term static, sustained, repeated, and dynamic. Dynamic loading includes loads from machines and from seismic events. Short-term static loading will lead to *p-y* curves that conceptually can be developed from properties of the supporting soil but do not occur often in practice. But *p-y* curves for short-term static loading are useful for cases where deflections are small and for sustained loading if the supporting soil is granular or overconsolidated clay. If sustained loading is present and the supporting soil is soft to medium clay, the engineer can expect that consolidation will occur. Lateral earth pressure can be computed, and the equations of consolidation can be applied to the extent possible. Installing a pile in the clay and imposing lateral loading, while observing deflection with time, is a useful procedure (Reuss et al., 1992).

Repeated and cyclic loading that will occur against an offshore structure is another matter. If deflection is small where the supporting soil is acting elastically, then the *p-y* curves for static loading may be used. For larger deflection, a significant loss of resistance will occur for overconsolidated clay and some for granular soil. If the mudline deflection of a pile is large enough that a gap will occur and if water exists at the site, erosion of overconsolidated clay will occur as water alternately falls into the gap and is squeezed out. The prediction of *p-y* curves for such a case does not readily yield to analysis but depends strongly on results from appropriate experiments. Figure 12.11a shows experimental *p-y* curves for cases of short-term static loading, and Figure 12.11b shows curves for cyclic loading for a pile in overconsolidated clay (Reese et al., 1975). The influence of cyclic loading on the *p-y* curves is apparent.

The *p-y* curves for short-term static loading can usually be used without modification for dynamic loading if deflections are very small. The prediction of *p-y* curves affected by earthquakes is a complicated problem. Some of the factors affecting the problem can be identified: the precise definition of the earthquake, the distance of the earthquake from the site, and the nature of the soils in the area of the site. The lateral and vertical accelerations at the site must be predicted utilizing the concept of microzonation. An earthquake in Mexico caused extensive damage in the Valley of Mexico, consisting of a deep deposit of clay, but the damage in the hills outside the Valley was

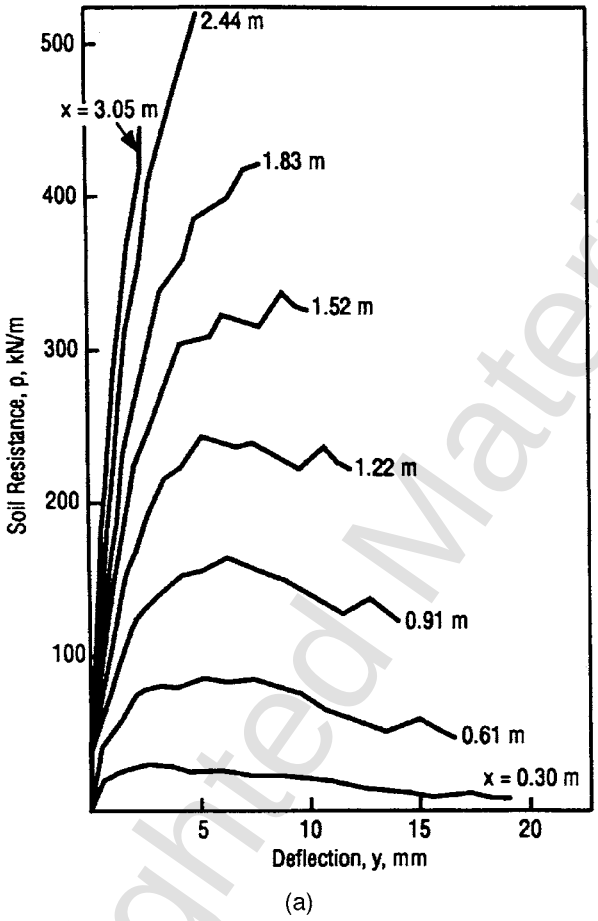

Figure 12.11 Lateral load test of an instrumented 24-in.-diameter pile: (a) *p-y* curves developed from a static load. (*Continued on page 398.*)

minimal. Along with accelerations of the ground surface, movements of the soil will occur as a function of depth. The *p-y* curves presented here do not include effects of inertia, nor are movements of the soil during earthquakes with respect to depth taken into account; therefore, the curves cannot be applied to an analysis of a pile-supported structure subjected to a seismic event without special consideration.

12.5 METHOD OF ANALYSIS FOR INTRODUCTORY SOLUTIONS FOR A SINGLE PILE

Engineers understood many years ago that the physical nature of some soils led to the argument that E_{py} should be zero at the mudline and increase

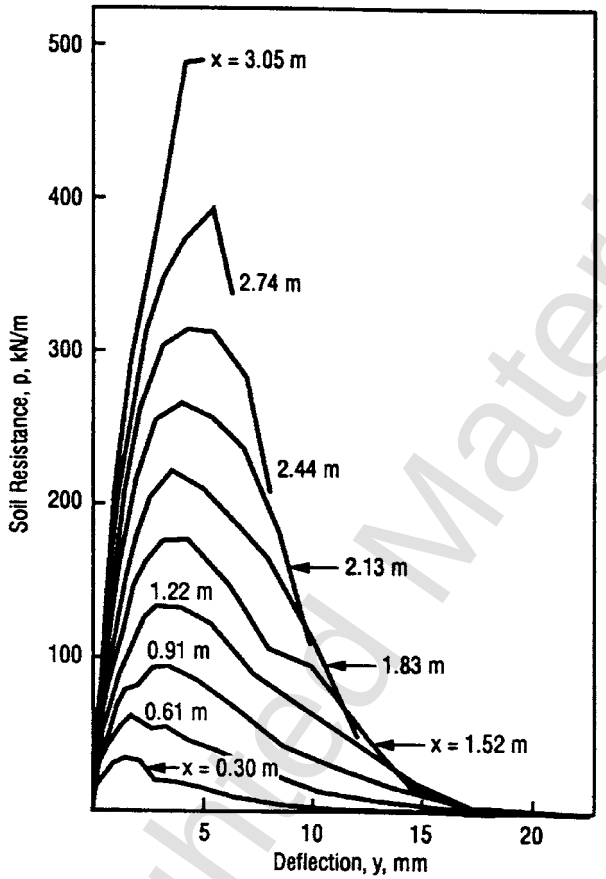

Figure 12.11 (*Continued*) (b) *p-y* curves developed from a cyclic load.

linearly with depth or that E_{py} is equal to $k_{py}x$. Granular soil and normally consolidated clays follow such a pattern and, even for overconsolidated clays, the value of the p_{ult} will be low near the ground surface. Therefore, crude but useful numerical solutions were made using hand-operated calculators, with the assumption that $E_{py} = k_{py}x$. Examination of the analytical parameters in the numerical solutions led to the proposal of a formal analytical procedure for $E_{py} = k_{py}x$ (Reese and Matlock, 1956) and later to the use of nondimensional methods to develop a wide range of solutions for a pattern of variations of E_{py} with depth (Matlock and Reese, 1962). While the availability of cheap and powerful personal computers has made rapid numerical solutions to Eq. 12.4 practical and inexpensive (see Chapter 14), reasons exist to present solutions for $E_{py} = k_{py}x$ where no axial load is applied ($p_x = 0$). The method

presents effectively the nature of the solution, yields the relationship between relevant parameters, and provides a useful method of solution for a range of practical problems.

The following equations can be developed by numerical analysis (Matlock and Reese, 1962) for the case where $E_{py} = k_{py}x$. A lateral load and a moment may be imposed at the pile head, and the length of the pile can be considered.

$$y = A_y \frac{P_t T^3}{E_p I_p} + B_y \frac{M_t T^2}{E_p I_p} \tag{12.46}$$

$$S = A_s \frac{P_t T^2}{E_p I_p} + B_s \frac{M_t T}{E_p I_p} \tag{12.47}$$

$$M = A_m P_t T + B_m M_t \tag{12.48}$$

$$V = A_v P_t + B_v \frac{M_t}{T} \tag{12.49}$$

$$T = \sqrt[5]{\frac{E_p I_p}{k_{py}}} \tag{12.50}$$

$$Z_{\max} = \frac{L}{T} \tag{12.51}$$

where

y, S, M, and V = deflection, slope, moment, and shear, respectively, along the length of the pile,

P_t and M_t = lateral load (shear) and applied moment at the pile head,

T = termed the *relative stiffness factor,* and

A_y, B_y, A_s, B_s, A_m, B_m, A_v, and B_v = nondimensional parameters shown in Figures 12.12 through 12.19.

The curves are entered with Z, where Z is equal to x/T. Because the soil is extending to the top of the pile, the distance below the ground surface z and the coordinate giving the distance along the pile from its head x are identical for this nondimensional method.

Several curves are shown in each of the figures where the nondimensional length of the pile is given. As may be seen in Figure 12.12, a pile with a nondimensional length of 2 exhibits only one point of zero deflection, with a

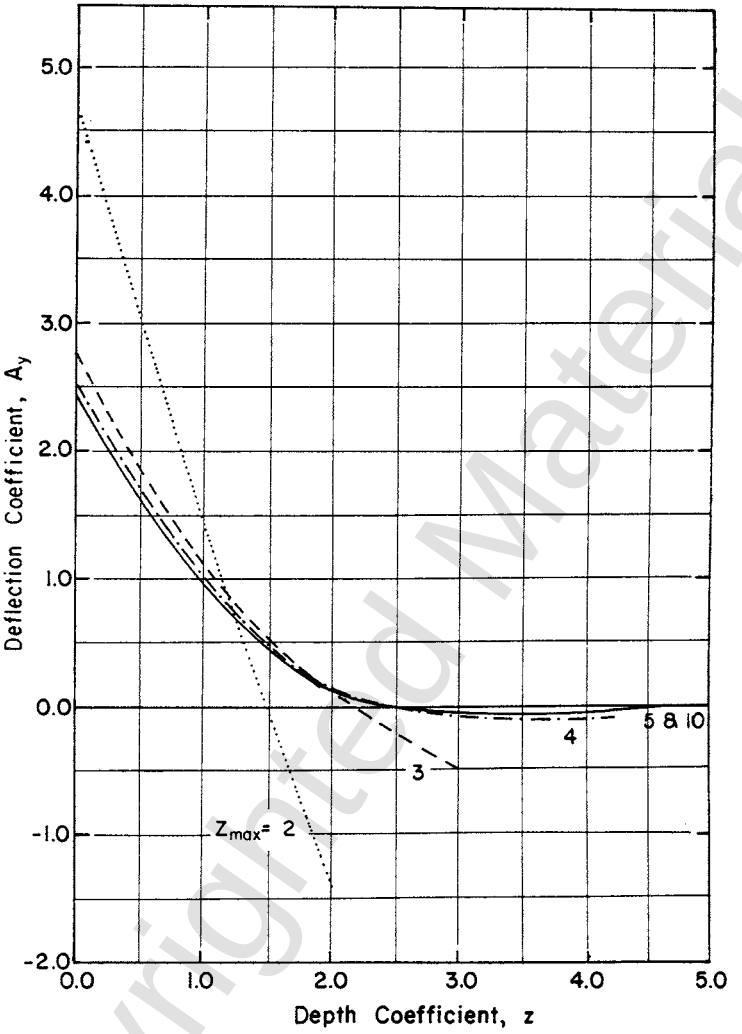

Figure 12.12 Pile deflection produced by a lateral load at the mudline.

substantial deflection of the bottom of the pile. In a number of practical cases, the embedded length of a pile is determined from the equations for axial resistance, and multiple points of zero deflection will appear during the analysis for lateral loading. If the length of the pile is dependent only on the response to lateral loading, piles are usually designed to have an embedded length to indicate two or three points of zero deflection. A ''short'' pile can behave like a fence post, typical of the case for a nondimensional length of 2.

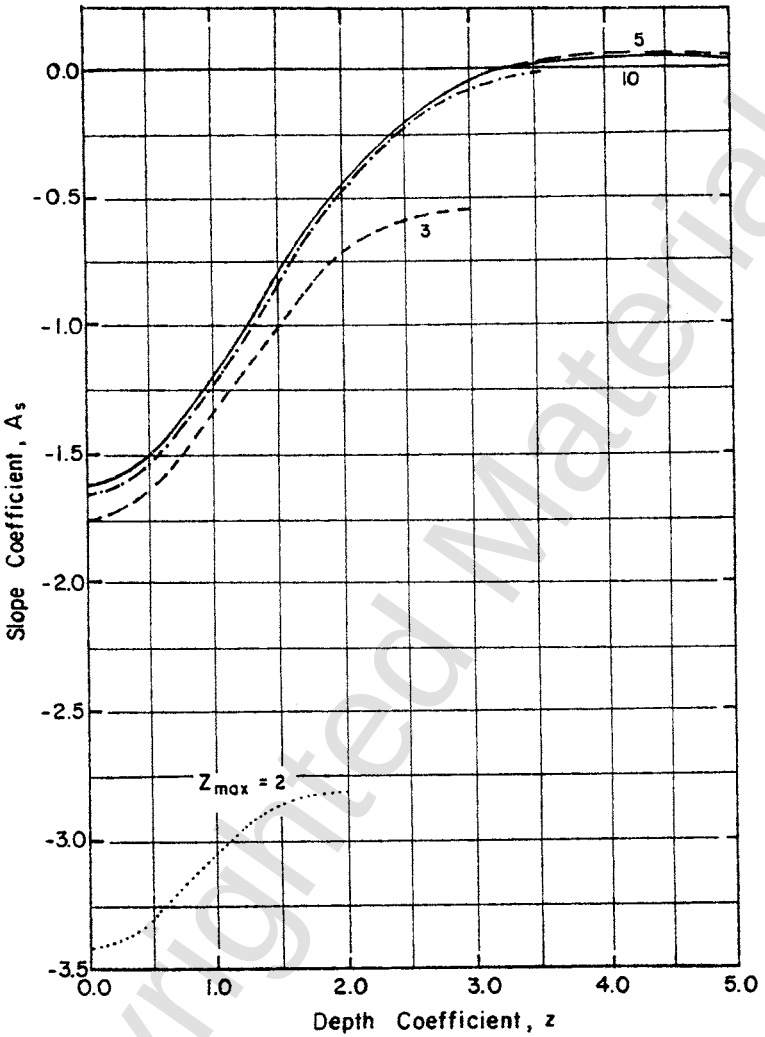

Figure 12.13 Slope of a pile caused by a lateral load at the mudline.

12.6 EXAMPLE SOLUTION USING NONDIMENSIONAL CHARTS FOR ANALYSIS OF A SINGLE PILE

A steel-pipe pile has been driven into the ground to serve as an anchor. A lateral load of 100 kN is to be applied to the top of the pile that is free to rotate. The load is increased to 300 kN to achieve an appropriate level of safety against failure of the pile where failure will occur with excessive bending. The magnitude of the deflection of the pile at the groundline is not judged to be critical.

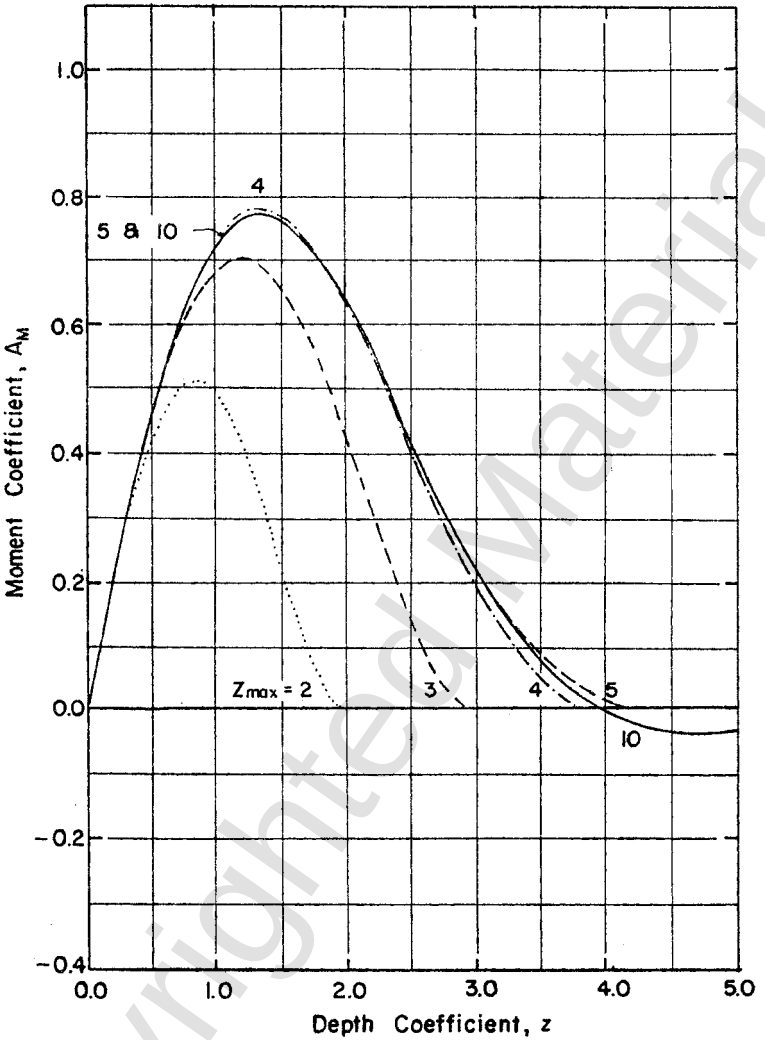

Figure 12.14 Bending moment produced by a lateral load at the mudline.

For purposes of the example, a steel pipe was selected with an outside diameter of 380 mm and an inside diameter of 330 mm. The moment of inertia I was computed to be 4.414×10^{-4} m^4, and the modulus of elasticity E was taken as 2.0×10^8 kPa, yielding the E_pI_p value of 88,280 kN-m^2. The yield strength of the steel was taken as 250,000 kPa, the stress at which a plastic hinge would occur. The length of the pipe was selected as 20 m.

A family of *p-y* curves was developed to represent the resistance of the soil to lateral loading, as shown in Figure 12.20. The curves are for an over-

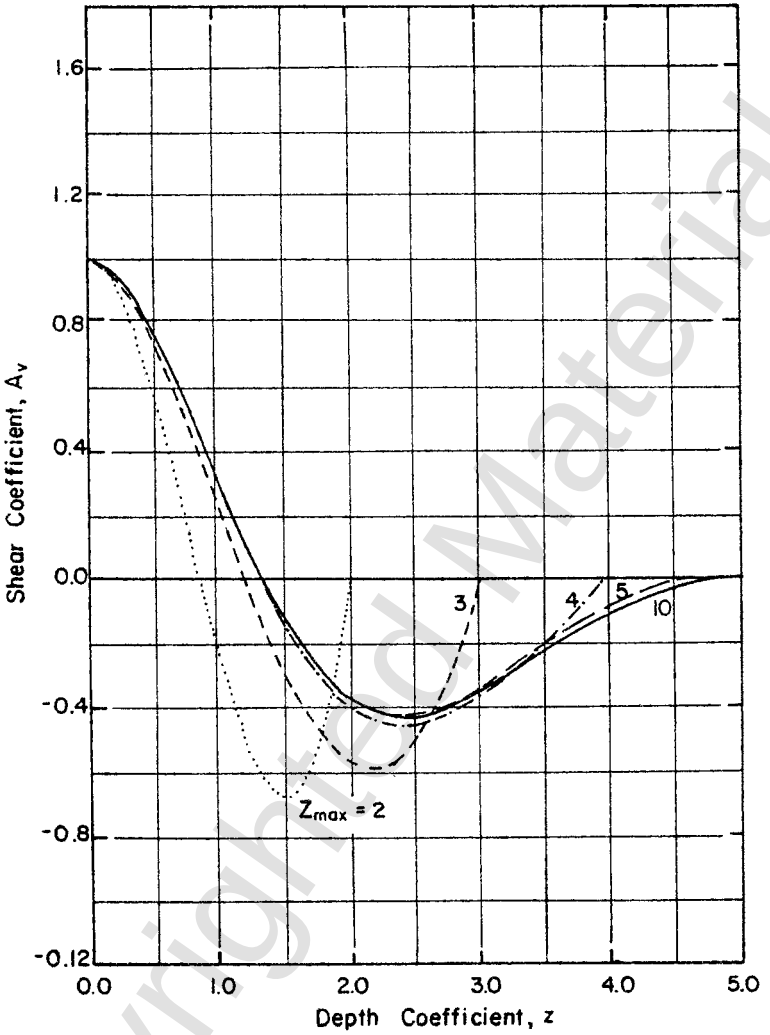

Figure 12.15 Shear produced by a lateral load at the mudline.

consolidated clay, assumed to be the soil at the site, for a pile with an outside diameter of 380 mm, and for the loading expected on the pile. Some aspects of the curves are instructive. For example, the initial portions of the curves form straight lines, representing a linear relationship between stress and strain. The initial portions of the curves show increased stiffness with depth, which is to be expected. The final portions of the curves are also straight lines, reflecting the fact that the deflection of the pile was sufficient to mobilize the full shear strength of the soil at the various depths. The *p-y* curve for the

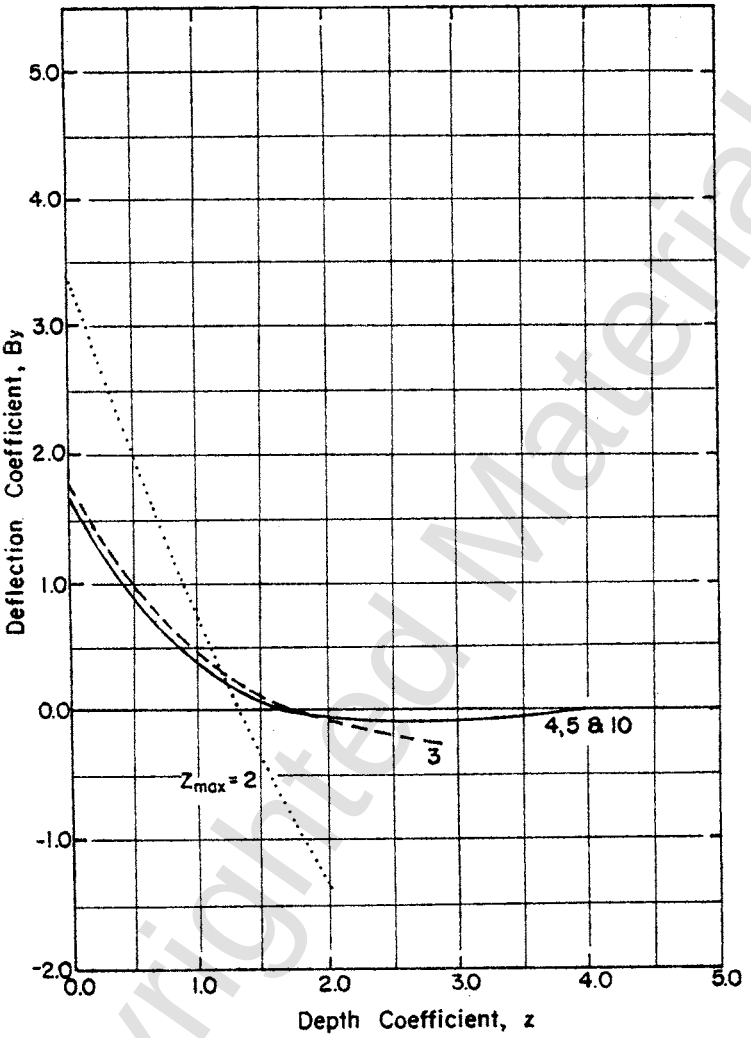

Figure 12.16 Pile deflection produced by moment applied at the mudline.

ground surface has some resistance; therefore, the assumption of $E_{py} = k_{py}x$ is not ideal for the example problem being solved. As noted earlier, the assumption that $E_{py} = k_{py}x$ should apply better to uniform sand or to normally consolidated clay.

Even though the nondimensional method is not ideally applied to the family of curves shown in Figure 12.20, the exercise that follows shows that useful results can be obtained when less than ideal *p-y* curves are used.

The procedure for a solution with the nondimensional method starts with (1) selection of the relative stiffness factor T (T_{tried}); (2) computation of $Z_{\max}$

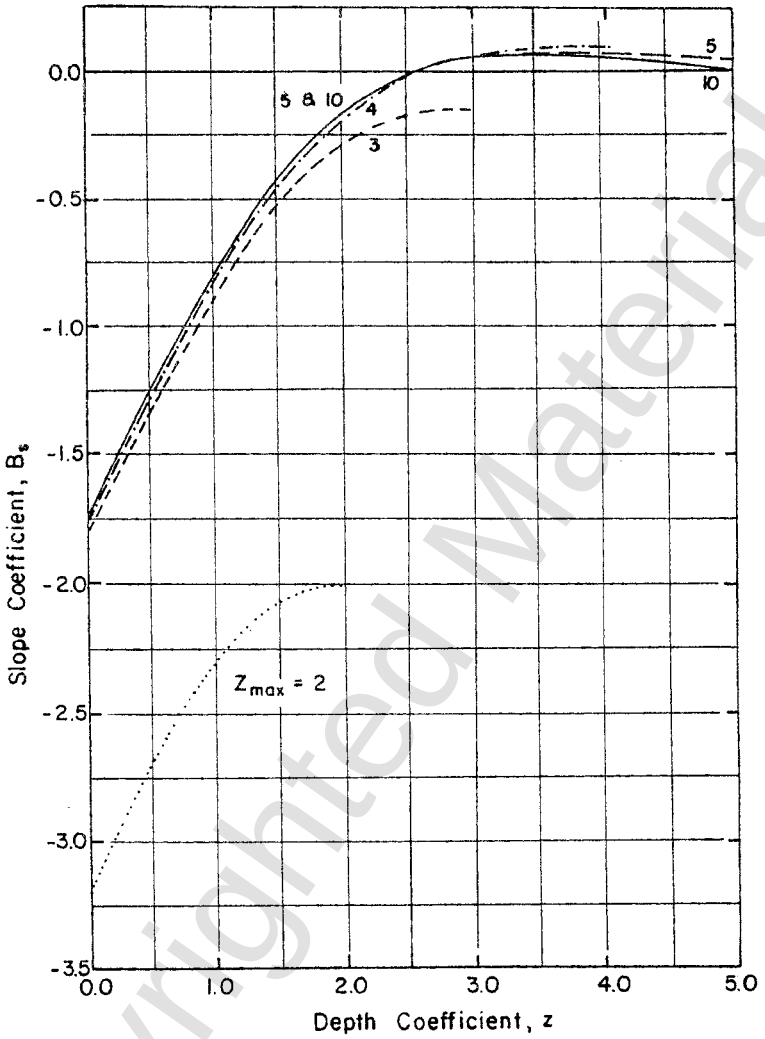

Figure 12.17 Slope of pile caused by moment applied at the mudline.

to select the curve to use in the nondimensional plots (Figures 12.12 through 12.19); (3) computation of a trial deflection of the pile using Eq. 12.46, selection of a corresponding value of p from Figure 12.20, computing E_{py} by dividing values of p by the corresponding values of y, plotting E_{py} as a function of x, fitting the best straight line from the origin through the plotted points to obtain the best value of k_{py}, where k_{py} is equal to E_{py} divided by x; and, finally, (4) computing a new value of T (T_{obt}) by using Eq. 12.50. If T_{obt} does not equal T_{tried}, a new value of T_{tried} is selected for a second trial. Two

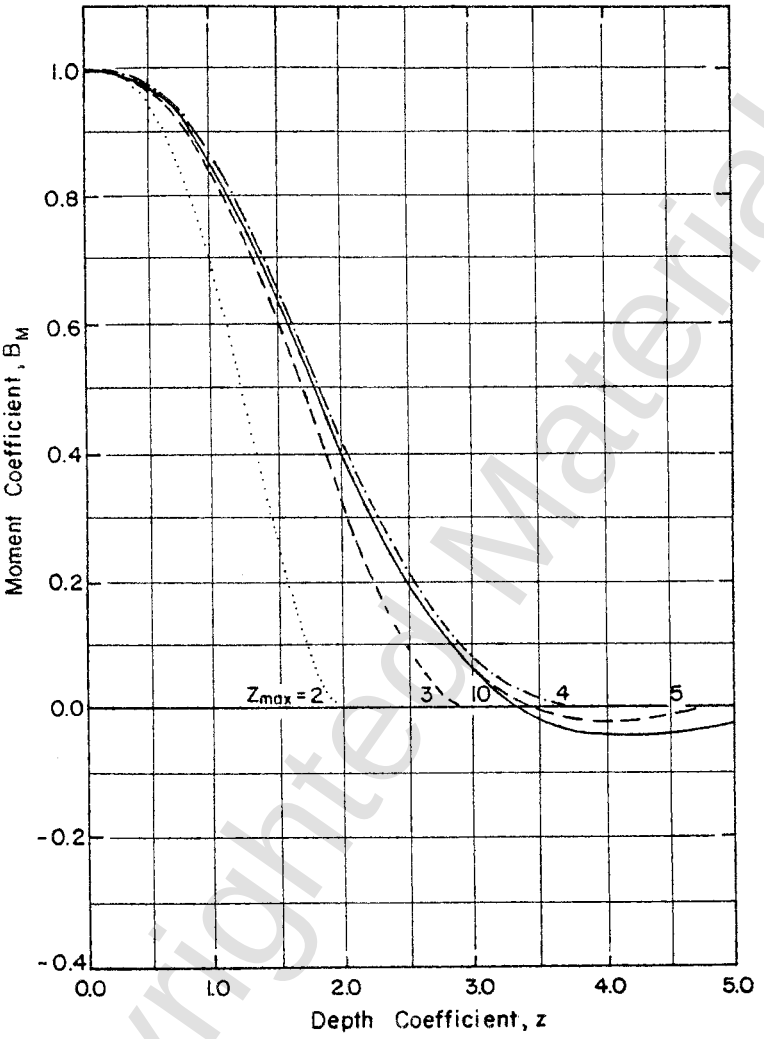

Figure 12.18 Bending moment produced by moment applied at the mudline.

trials are frequently sufficient to obtain convergence, where successive trials are necessary to accommodate the nonlinearity of the problem.

Try T = 2 m, $Z_{\max} = \dfrac{L}{T} = 10$; use the appropriate curve for A_y in Figure 12.12.

$$y_A = A_y \frac{P_t T^3}{E_p I_p} = A_y \frac{(300)(2^3)}{88{,}280} = A_y(0.027186) \text{ m} = A_y(27.186) \text{ mm}$$

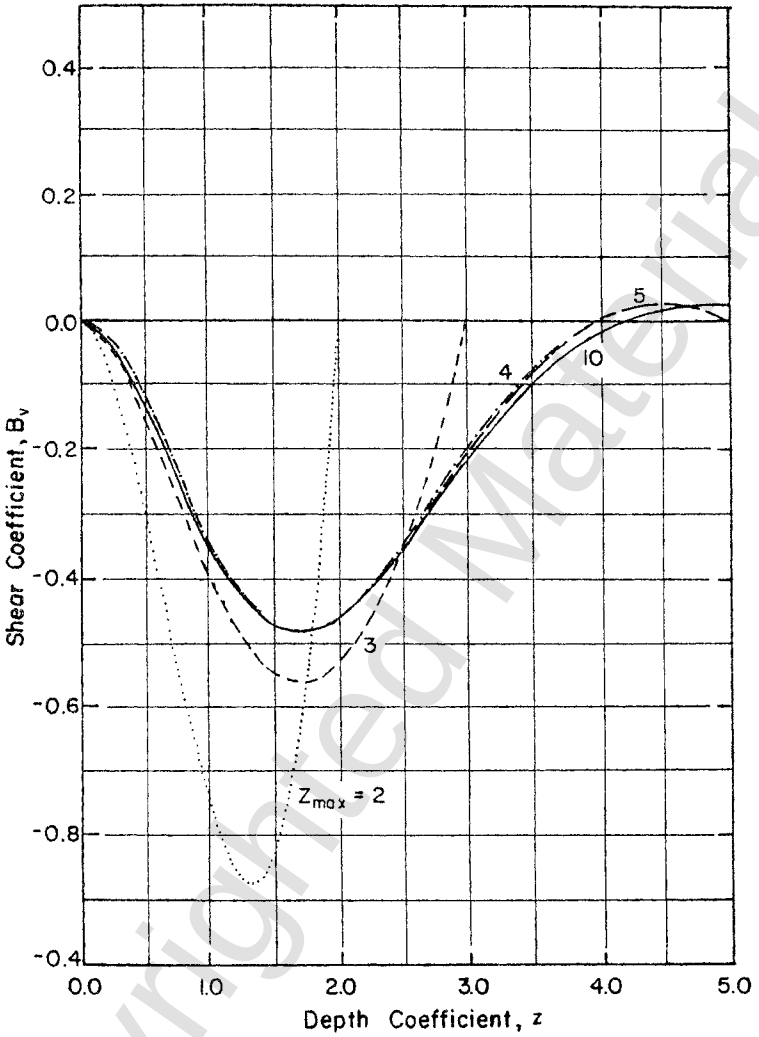

Figure 12.19 Shear produced by moment applied at the mudline.

x, m	Z	A_y	y_A, mm	p, kN/m	E_{py}, kPa
0	0	2.435	66.2	110	1,662
0.25	0.125	2.2	59.8	107	1,789
0.51	0.255	2.0	54.4	115	2,114
1.02	0.51	1.6	43.5	133	3,057
1.78	0.89	1.1	29.9	150	5,017
2.54	1.27	0.7	19.0	162	8,526
3.81	1.91	0.15	4.1	140	34,146

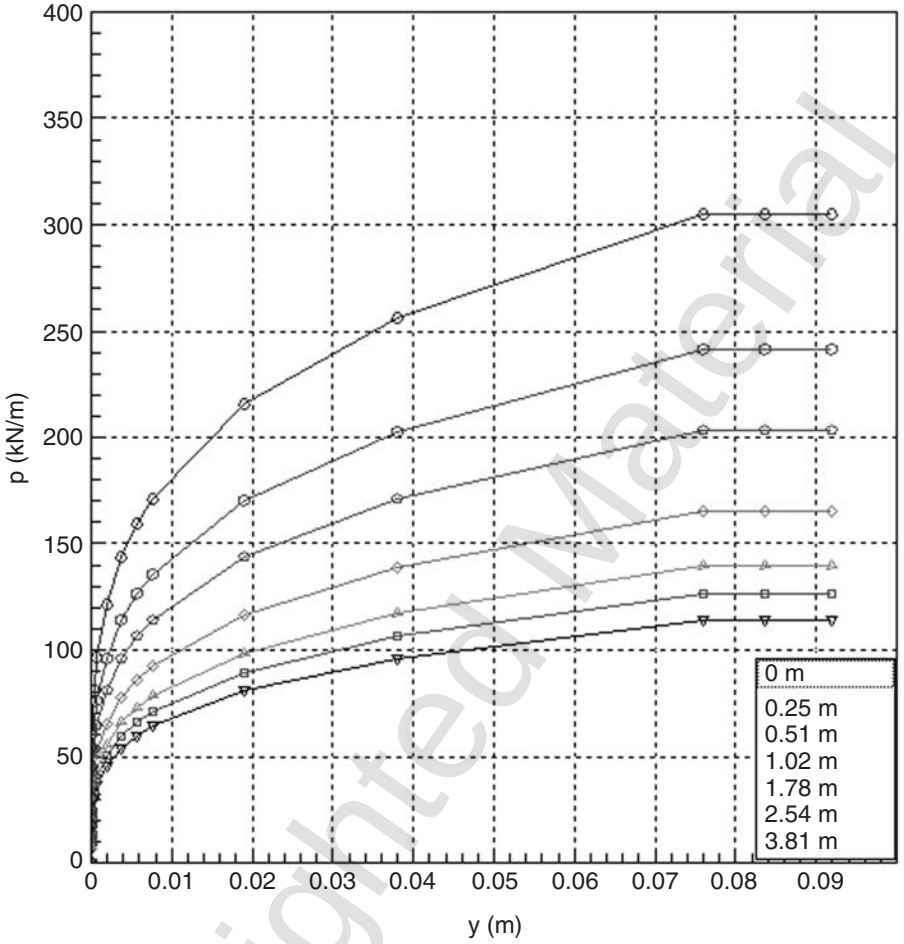

Figure 12.20 Family of *p-y* curves for an example problem.

The derived values of E_{py} versus x for a value of T of 2.0 are plotted in Figure 12.21. A straight line is plotted that passes through the origin. As can be seen, the first three points are on the right side of the line, the next two are on the left side, and the final point is on the right side. Even though the line seems to be a poor fit of the data points, the results are useful. The computations show that the slope of the line was employed to find an obtained value of T, a value of 1.91 m.

Because the value of T_{obt} was lower than that of T_{tried}, the second trial was made with a T_{tried} value of 1.5 in order to limit the number of trials to achieve convergence. The computations proceeded as before. The new value of T led

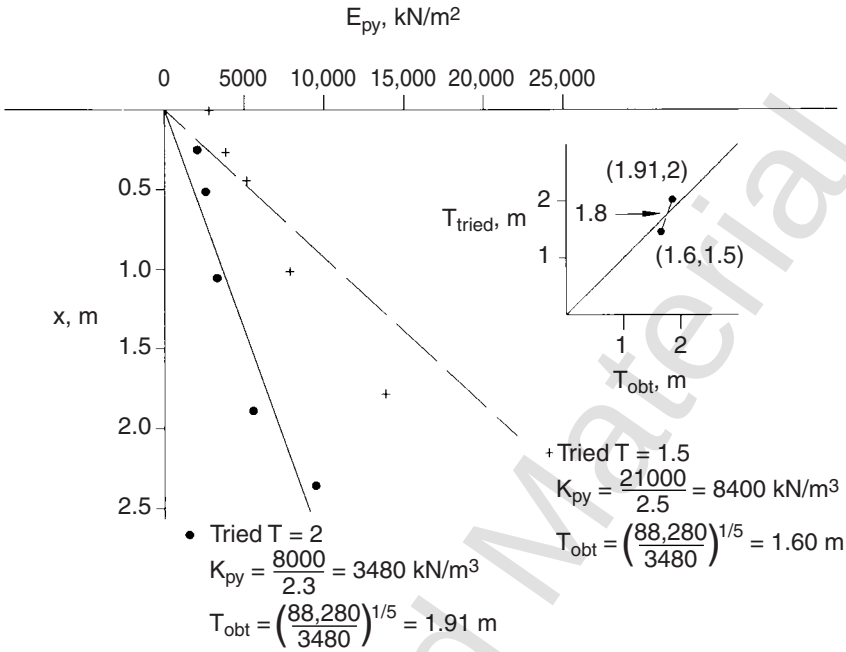

Figure 12.21 Graphical solution for the relative stiffness factor for an example problem.

to new values of Z and A_y, and hence to new values of p and E_{py}. The plotted results are shown in Figure 12.21, where the value of T_{tried} of 1.5 m led to a value of T_{obt} of 1.60 m. The values of the relative stiffness factor tried and obtained are plotted in the sketch in Figure 12.21. As shown in the plot, convergence occurred at a value of T of 1.80 m.

The response of the pile under the lateral load of 300 kN can now be computed using the first terms in Eqs. 12.46 and 12.48. After computing $Z_{\max}$, the curves to use in Figs. 12.12 and 12.14 may be selected.

$$Z_{\max} = 20/1.8 = 11.1$$

so use the curves for $Z_{\max} = 10$.

$$y = A_y P_t T^3 / E_p I_p = A_y \frac{(300)(1.8^3)}{88,280} = A_y\ (0.01982)\ \text{m} = A_y\ (19.82)\ \text{mm}$$

$$M = A_m P_t T = A_m\ (540)\ \text{kN-m}$$

Z	x, m	A_y	y, mm	A_m	M, kN-m
0	0	2.4	47.6	0	0
0.5	0.9	1.6	31.7	0.46	248
1.0	1.8	0.9	17.8	0.72	389
1.5	2.7	0.4	7.9	0.76	410
2.0	3.6	0.2	4.0	0.64	346
2.5	4.5	0	0	0.41	221
3.0	5.4	−0.05	−1.0	0.22	119
4.0	7.2	−0.05	−1.0	0	0
5.0	9.0	0	0	−0.04	−22

$$f_{\max} = \frac{(410)\left(\dfrac{0.38}{2}\right)}{4.414 - 10^{-4}} = 176{,}500 \text{ kPa} < 250{,}000$$

As the above computation shows, the load factor of 3 led to a computed bending stress less than that required to cause a plastic hinge. The computed values of deflection and bending moment are plotted in Figure 12.22. The digital computer was used to solve the problem with the method presented in

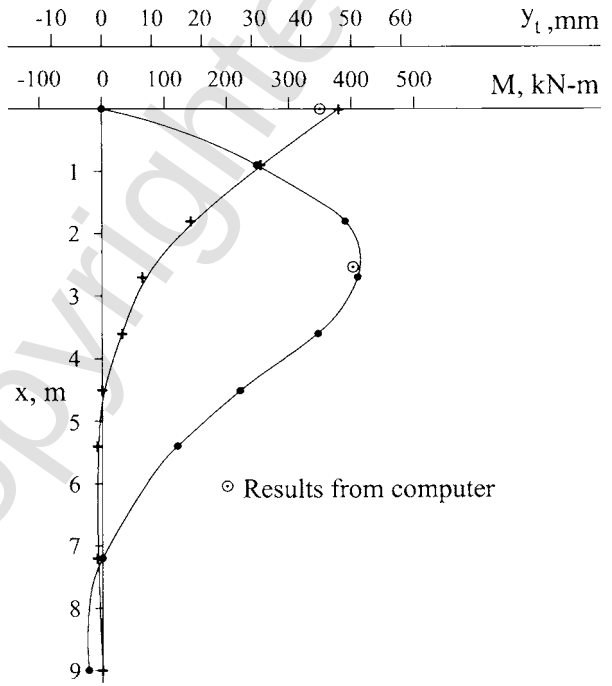

Figure 12.22 Computed values of deflection and maximum bending moment for an example problem.

Chapter 14, and the results for maximum bending moment and groundline deflection are plotted in Figure 12.22. While the computer gave a value of groundline deflection about 10% lower than the value from the nondimensional method, the position and magnitude of the maximum bending moment of the computer solution agreed closely with the results of the nondimensional method.

The deflection at the groundline of 47.6 mm may be considered excessive even though the lateral load had been factored up. At one time, excessive deflection at the groundline caused some investigations to speculate that there had been a ''soil failure,'' but the soil does not actually fail; the deflection becomes excessive only for some applications. For the case analyzed, the designer might wish to make a computation without factoring up the load to obtain an idea of the deflection under the working load.

Several comments are pertinent concerning the solution obtained with the nondimensional method with the assumption that $E_{py} = k_{py}x$.

1. The values of deflection for the top of the pile obtained with the nondimensional method and the computer are in reasonable agreement. The values of maximum bending moment achieved agree almost exactly, both in regard to value and to location. One could reason that the good agreement between the results is only accidental, but close agreement has also been found when other problems are solved with both methods.
2. Compared with the computer solution, the nondimensional method is time-consuming and tedious because values must be estimated from curves and the nonlinearity of the problem requires iteration.
3. However, the nondimensional method is valuable because a computer solution can be checked, which may be required in some cases, and because the hand solution gives the beginning user an excellent introduction to a fairly complex problem.
4. The nondimensional method is limited in that no axial load may be imposed, the pile stiffness must be constant with depth and independent of the bending moment, and the method is not applicable to layered soils. All of these limitations are overcome by the methods shown in Chapter 14.

PROBLEMS

P12.1. List examples of piles under lateral loading in the community where you live and sketch one example, showing rough dimensions and the source of lateral loading, along with a note showing the condition of the soil at the ground surface.

P12.2. For the solved example in the section on nondimensional solutions, compute the deflection at the top of an unloaded extension of the pile to a height of 5 m.

P12.3. **a.** For the pile and *p*-*y* curves used in the example in the nondimensional method of solution, work out the case where the pile is loaded with a horizontal load of 65 kN at 8 m above the groundline, yielding a value of P_t of 65 kN and a value of M_t of 520 kN-m. Solve for the value of T_{obt} with values of T_{tried} assigned by the instructor.

b. Bring your values of T_{tried} and T_{obt} to class to make a plot to find the value of T where the solution converges.

c. Using the value of T found in (b), make a plot of pile deflection y and bending moment M as a function of length along the pile. Compute the value of the maximum bending stress and compare it with the stress that will cause a plastic hinge.